Quart. J. R. Met. Soc. (1978), **104**, 699–718

551.521.3

Spectral distribution of solar radiation. I: direct radiation

By H. A. McCARTNEY* and M. H. UNSWORTH

Department of Physiology and Environmental Studies, School of Agriculture, Nottingham University, Sutton Bonington, Loughborough

(Received 14 February 1977; revised 28 November 1977)

SUMMARY

Measurements of the spectral distribution of direct solar radiation, made in both wide and narrow wavebands, are reported. The measurements suggest that the wavelength dependence of aerosol attenuation in central England, in summer, can generally be described by a power law with wavelength exponent of about 1·7. Attenuation of visible radiation is reported in terms of an integral turbidity coefficient, τ_v, and is shown to depend to some extent on air mass origin, air masses from the continent being more turbid than maritime air masses. The mean value of τ_v is 0·31 with a range of 0·05 to 0·6. The ratio of visible to total direct irradiance is found to be a linear function of τ_v, the constants of linearity being functions of zenith angle. From these relationships a semi-empirical model is developed enabling spectral irradiance, visible irradiance and total solar irradiance to be estimated from arbitrary values of turbidity and zenith angle.

1. INTRODUCTION

In recent years requests have come from biologists, from physicists, and from engineers for more information concerning the quantity and quality of solar radiation reaching the earth's surface. The spectral distribution of solar radiation can be discussed in terms of broad wavebands (e.g. visible 300–700 nm) or narrow wavebands (1–10 nm). For studies of radiant energy exchange between biological systems and their surroundings wideband spectral distributions are generally adequate. Other biological light-stimulated processes require more detailed knowledge of the spectral distribution of radiant energy for their evaluation; for example, vision in animals and photosynthesis in plants. Increasing awareness of the depletion of non-renewable energy sources has stimulated investigations into new methods of converting solar energy into useful power. To evaluate some of these methods only wideband spectral information is required. However, systems involving photoelectric or photovoltaic processes require narrowband spectra for their appraisal.

Solar radiation reaches the earth's surface either directly or after being scattered by atmospheric molecules or particles. This paper reports measurements, in central England, of the spectral irradiance of the direct solar beam and analyses the effects of airborne particles (aerosols) on the spectral distribution. Measurements of the spectral distribution of scattered and global radiation will be dealt with in a subsequent paper.

The spectral distribution of solar radiation was first investigated quantitatively by Langley (1881), but there have been few systematic investigations of direct-beam spectral irradiance in spite of reports of changes in atmospheric transmission during the twentieth century (McCormack and Ludwig 1967; Hodge 1971). Moon (1940) published a series of spectral energy curves calculated from available estimates of atmospheric attenuation. Other authors have reported examples of calculated spectral distributions based on various model atmospheres (Gates 1966; Unsworth and McCartney 1973; Dave, Halpern and Braslau 1975). Measured narrowband spectra have also been published, both in energy units (Dunkelman and Scolnik 1959; Randerson 1970) and in chromaticity (Taylor and Kerr 1941).

Investigations of spectral distributions using wideband cut-off filters have been

* Present address: Dept. of Environmental Sciences, University of Lancaster, Bailrigg, Lancaster.

reported from several sites: Blackwell, Eldridge and Robinson (1954) from Kew, England; Drummond and Ångstrom (1967) from Hawaii; and Kuhn (1972) from Antarctica. Since the work of Blackwell *et al.* little attention has apparently been paid to the spectral quality of the components of solar radiation in the United Kingdom apart from the relative spectral distributions of global (sun and sky) radiation reported by Henderson and Hodgkiss (1963). As part of a biological study, the spectral distribution of solar radiation in both wide and narrow wavebands was undertaken at the School of Agriculture, University of Nottingham, Sutton Bonington (52·8°N 1·25°W), during the summers of 1972 and 1973.

2. Theoretical considerations

The attenuation of monochromatic radiation in the direct beam by the atmosphere may be described by a Lambert–Beer equation of the type

$$I(\lambda) = I_0(\lambda)\exp[-\{\tau_R(\lambda)+\tau_g(\lambda)+\tau(\lambda)\}m] \quad . \quad . \quad (1)$$

where $I(\lambda)$ and $I_0(\lambda)$ are respectively the spectral irradiance below and above an atmosphere in which $\tau_R(\lambda)$, $\tau_g(\lambda)$ and $\tau(\lambda)$ are respectively the vertical attenuation coefficients for molecular scattering, absorption by atmospheric gases (water vapour, carbon dioxide, ozone, oxygen), and aerosol extinction; and m, the air-mass number, is the number of equivalent vertical paths traversed. For most solar zenith angles, Z, m is well approximated by $\sec(Z)$ for each attenuator although it may be noted that m need not necessarily be the same for each atmospheric constituent (Robinson 1966).

Molecular attenuation coefficients $\tau_R(\lambda)$, calculated from Rayleigh's theory, were tabulated by Penndorf (1957) and Elterman (1968) and evidence supporting the accuracy of the theory has been reported by Fowle (see Moon 1940). In an extensive laboratory study, which has become a standard source of data, Howard, Burch and Williams (1955) examined the spectral absorption of the main atmospheric gases. Attenuation coefficients for these gases may be derived from their results and knowledge of atmospheric composition. The integrated effect of gaseous absorption on the attenuation of solar radiation has been investigated by several authors (McDonald 1960; Roach 1961; Yamamoto 1962).

Spectral attenuation of solar radiation by atmospheric aerosols depends on the nature and concentration of the aerosol particles. The mathematical theory of particle attenuation of monochromatic radiation was first formulated by Mie (1908) (see Van de Hulst 1959 or Kondratyev 1969) and tables of extinction cross-sections for particles of various sizes and refractive indices are available (Penndorf 1956; Diermendjian, Clasen and Viezee 1961; Diermendjian 1963; Kattawar and Plass 1967). Vertical attenuation coefficients have been calculated for various aerosol size distributions and refractive indices (Valko 1961; Barnhardt and Streete 1970; Bergstrom 1972; Unsworth and McCartney 1973) and it has been shown (Valko 1961; McCartney 1975) that many common size distributions yield relationships similar to an empirical equation first proposed by Ångstrom (1929 and 1930):

$$\tau(\lambda) = \gamma\lambda^{-\alpha} \quad . \quad . \quad . \quad . \quad (2)$$

γ and α being constants.

When wavelength is measured in micrometres the value of γ corresponds to the attenuation coefficient at 1 μm and this value has sometimes been used as an index of atmospheric turbidity (Ångstrom's turbidity coefficient β, Ångstrom 1964). In the present study it was more convenient when measuring wavelengths in nanometres to study the spectral turbidity at 500 nm, i.e.

$$\tau(500) = \gamma 500^{-\alpha} \quad . \quad . \quad . \quad . \quad (3)$$

TABLE 1. SPECTRAL IRRADIANCE FOR A 'CLEAN' ATMOSPHERE, $I_*(\lambda)$, AS A FUNCTION OF WAVELENGTH, λ

Wavelength (nm)	Irradiance ($W m^{-2} nm^{-1}$) $Z = 0°$	$Z = 20°$	$Z = 40°$	$Z = 60°$	$Z = 80°$
300	0·007	0·005	0·002	0·000	0·000
320	0·243	0·224	0·167	0·071	0·001
340	0·513	0·489	0·409	0·245	0·015
360	0·607	0·585	0·511	0·345	0·041
380	0·714	0·694	0·622	0·455	0·084
400	0·993	0·970	0·889	0·690	0·176
420	1·296	1·271	1·182	0·961	0·313
440	1·420	1·398	1·318	1·113	0·448
460	1·680	1·658	1·577	1·366	0·628
480	1·734	1·714	1·642	1·450	0·741
500	1·660	1·643	1·582	1·419	0·787
520	1·595	1·581	1·529	1·388	0·824
540	1·566	1·553	1·505	1·375	0·844
560	1·493	1·481	1·436	1·315	0·817
580	1·513	1·501	1·457	1·336	0·836
600	1·487	1·476	1·436	1·326	0·865
620	1·455	1·446	1·413	1·322	0·922
640	1·428	1·421	1·395	1·321	0·986
660	1·392	1·387	1·365	1·305	1·023
680	1·348	1·344	1·326	1·278	1·047
700	1·309	1·305	1·291	1·251	1·057
720	1·265	1·262	1·250	1·218	1·056
740	1·218	1·215	1·206	1·178	1·037
760	1·175	1·173	1·165	1·142	1·026
780	1·129	1·128	1·143	1·102	1·003
800	1·084	1·083	1·077	1·061	0·981

Calculated for an atmosphere containing 0·35 cm of ozone using the extraterrestrial spectrum of Thekaekara (1971) and the Rayleigh and ozone attenuation coefficients of Elterman (1968).

The turbidity coefficient, B, proposed by Schüeppe (1949) and used extensively (Volz 1969; Kuhn 1972; Hansen 1973) is related to $\tau(500)$ by $\tau(500) = 2{\cdot}303B$.

Many experimental investigations have confirmed Eq. (2) (Curcio 1961; Irvine and Peterson 1970) with exponent α between 0 and 2 but others have found different variations of attenuation with wavelength (Quenzel 1970; Barnhardt and Streete 1970; Vittori, Tomasi and Guzzi 1974) and have found particularly that attenuation spectra followed a power law at visible wavelengths but flattened or dipped in the infrared (Knestrick, Cosden and Curcio 1962; Yamamoto and Tanaka 1969). Rensch and Long (1970) attributed this, in high relative humidity, to the change in refractive index of water with wavelength, but the phenomenon may also occur at low relative humidity when aerosols absorb at infrared wavelengths.

In the waveband 300–800 nm absorption of radiation by atmospheric gases, primarily ozone, varies little compared with aerosol attenuation and so it is convenient to rewrite Eq. (1) as

$$I(\lambda) = I_*(\lambda)\exp[-\tau(\lambda)m] \quad . \quad . \quad . \quad (4)$$

where $I_*(\lambda)$ is the radiation emerging from an aerosol-free atmosphere. Table 1, which was calculated using the ozone and Rayleigh attenuation coefficients of Elterman (1968) and extraterrestrial irradiance of Thekaekara (1971), shows $I_*(\lambda)$ for several values of air-mass.

Wideband direct beam solar irradiance can be similarly analysed in terms of aerosol attenuation (turbidity). Unsworth and Monteith (1972) used an integral turbidity coefficient, $\tau(\Delta\lambda)$, to describe aerosol attenuation in a finite waveband, $\Delta\lambda$. By analogy to Beer's law (Eq. (1))

$$I(\Delta\lambda) = I_*(\Delta\lambda)\exp[-\tau(\Delta\lambda)m]$$
$$\tau(\Delta\lambda) = [\ln\{I_*(\Delta\lambda)\} - \ln\{I(\Delta\lambda)\}]/m \quad (5)$$

where $I(\Delta\lambda)$ is the direct irradiance in the waveband $\Delta\lambda$ and $I_*(\Delta\lambda)$ is the irradiance emerging from an aerosol-free atmosphere (Unsworth and McCartney 1973). Integral turbidity coefficients are easily calculated especially when the wavebands are free from selective absorption by atmospheric gases.

The variation of aerosol attenuation coefficients with wavelength (e.g. Eq. (2)) means that if Beer's law is applied to a finite waveband then $\tau(\Delta\lambda)$, in Eq. (5), becomes a function of air-mass as well as of aerosol concentration. However, the relative magnitudes of integral turbidity coefficients, at constant air-mass, depend only on the variation of $\tau(\lambda)$ with λ and on aerosol concentration. Using a simplified model atmosphere and assuming power-law attenuation by aerosol (Eq. (2)), McCartney (1975) calculated integral turbidity coefficients for the commonly measured wavebands, 300–630 nm (τ_r), 300–710 nm (τ_v) and 300–3000 nm (τ_t), as functions of the power-law exponent α and air-mass m. The ratios τ_r/τ_v and τ_t/τ_v, for fixed α and m were found to be independent of τ_v in the range $0{\cdot}0 < \tau_v < 0{\cdot}5$. Fig. 1 shows the variations of τ_r/τ_v and τ_t/τ_v with α and m. The figure shows that it is possible to estimate α by measuring the ratio of integral turbidities in different wavebands. An example of such an estimation is given in section 4(*b*).

3. Instrumentation and measurements

(*a*) *Narrowband measurements*

Direct spectral irradiance, $I(\lambda)$, was measured in the waveband interval 400–800 nm using a model 2000 spectroradiometer manufactured by Gamma Scientific Inc., California.

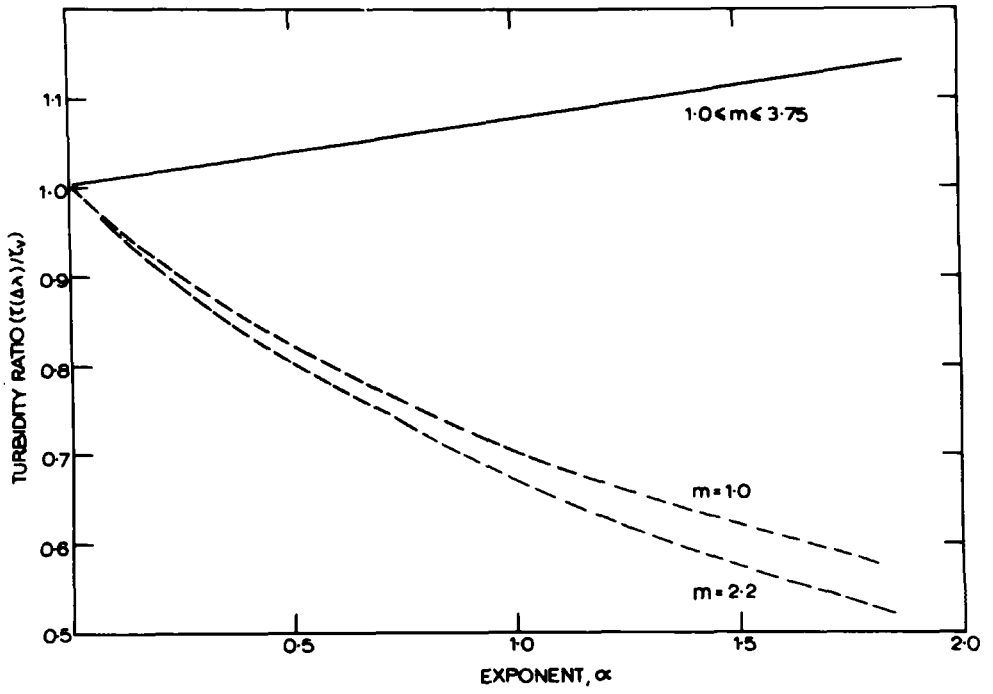

Figure 1. Turbidity ratio $(\tau(\Delta\lambda)/\tau_v)$ as a function of wavelength exponent, α, and air-mass m. —— τ_r/τ_v; --- τ_t/τ_v.

Radiation entered the instrument via a miniature head of diameter 0·25 cm attached to a 3·3 m fibre-optic light guide with a rectangular exit aperture matched to the entrance slit of the monochromator. Transmission of the fibre-optics lead was strongly wavelength dependent at wavelengths less than 450 nm.

Light dispersion in the monochromator was achieved by a single diffraction grating (1350 lines cm^{-1}). For all measurements the exit and entrance slits were set to give a spectral bandwith of 8 nm. Spectral scanning was achieved by a variable speed electric motor. Second-order diffraction was eliminated automatically by inserting a shortwave cut-off filter into the diffracted beam at wavelengths greater than 600 nm. The radiation was detected by a photomultiplier tube with an S1 cathode. Photomultiplier current was converted to voltage, amplified and displayed on the y axis of an x–y recorder, while a voltage signal, proportional to the wavelength, was displayed on the x axis of the recorder. A complete spectrum could be measured in about 15 seconds. The graphical output produced was converted manually to digital form for computer processing.

The spectroradiometer system was calibrated in two ways. In the laboratory, light from a tungsten halogen lamp, calibrated by the National Physical Laboratory, was used to calibrate the whole system, giving a set of calibration coefficients to convert the amplifier output to absolute irradiance units ($W\,m^{-2}nm^{-1}$). In the field, using direct solar radiation as a source, comparisons were made between measurements made with a Linke–Feussner pyrheliometer fitted with RG 695 and RG 630 Schott glass filters (formerly RG 8 and RG 6) (isolating, by difference, irradiance in the 630–710 nm waveband) and the integrated output of the spectroradiometer in the same waveband. The shortwave cut-off for each filter was measured using a spectrophotometer and found to be 710 nm for the RG 695 and 630 nm for the RG 630 filter.

The frequent calibrations during the period of measurement showed that the wavelength response of the spectroradiometer was constant with time but the sensitivity decreased, probably as a result of broken fibres in the fibre-optic light guide.

Direct spectral irradiance was measured by fitting the detector head to a collimator, a plain metal tube painted internally with Parson's optical black lacquer, which subtended an angle of 1°. The collimator was aimed at the sun using a small optical sight, the accuracy of which was frequently checked by moving the collimator to confirm that the photomultiplier output was a maximum.

(*b*) *Wideband measurements*

Direct solar irradiance in several wavebands was measured using the Linke–Feussner pyrheliometer. The instrument, described in detail by Robinson (1966), has a series of collimating diaphragms designed to accept radiation within a cone of half angle 5·1°. Thus when directed at the solar disc, which subtends an angle of 0·5°, the instrument records radiant energy in the direct beam with a relatively small addition from a small area of sky around the sun (Ångstrom and Rodhe 1966).

Separation of the spectral bands was achieved by inserting RG 695 and RG 630 Schott glass filters into the direct beam. The filters enable direct irradiance, $I(\Delta\lambda)$, to be determined in the following spectral regions:

Total, I_t, 300–3000 nm; visible, I_v, 300–710 nm and I_r, 300–630 nm.

As the response time of the instrument was about 8 seconds a full set of measurements could be taken in about one minute.

The pyrheliometer was calibrated at the World Radiation Center, Davos, in January 1972, against an Ångstrom pyrheliometer using the sun as source. Comparison during 1973 and 1974 with a Kipp solarimeter, kept solely for this purpose, showed that there was no

detectable change in calibration during the series of measurements. The filter reduction factors, used when correcting for absorption and reflection, were estimated from the spectral transmission function of the filter, measured using a spectrophotometer, and from solar spectral irradiance curves of Avaste, Moldau and Schifrin (1962) computed from a programme by Szeicz (personal communication).

4. Results

Measurements of both narrowband and wideband direct spectral irradiance were made at Sutton Bonington during the summer of 1973; wideband measurements only were made during 1972.

(*a*) *Narrowband results*

One hundred and six observations of direct solar spectra (400–800 nm) were taken under approximately clear sky conditions (< 1/8 cloud with no cloud near the sun) for a range of zenith angles of 30–70°. As this spectral interval is virtually free of significant molecular absorption, except for ozone, it was possible to calculate aerosol attenuation coefficients, $\tau(\lambda)$, for each spectrum. The coefficients, integrated over an interval of 20 nm, were calculated using the extraterrestrial irradiance, $I_0(\lambda)$, of Thekaekara (1971) and the Rayleigh and ozone attenuation coefficients of Elterman (1968). Mean monthly values of atmospheric ozone concentration for the latitude of the site were taken from Robinson (1966).

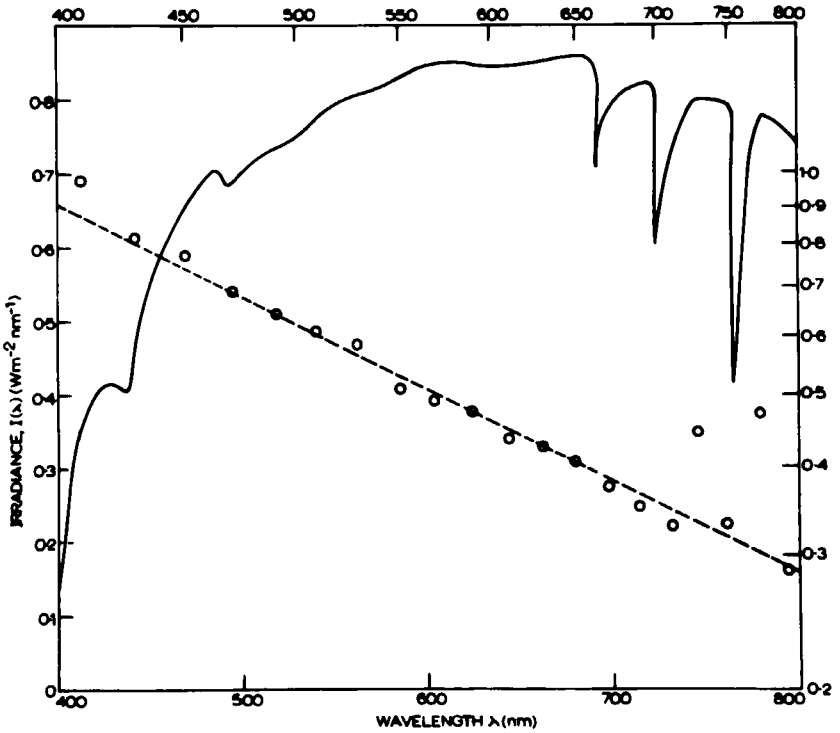

Figure 2. Spectral irradiance and spectral turbidity for 1135 GMT on 16 August 1973. ——spectral irradiance $\mathrm{W\,m^{-2}nm^{-1}}$; ○, spectral turbidity, $\tau(\lambda)$; ----- linear regression through $\log(\tau(\lambda))$ *v.* $\log(\lambda)$ (top and right-hand scales).

Almost all (104) of the spectral turbidity coefficients were reasonably well fitted by a power law (Eq. (2)). Fig. 2 shows an example of a typical spectrum measured on 16 August 1973 at 1135 GMT ($Z = 39{\cdot}5°$, $m = 1{\cdot}3$). Also shown is $\log(\tau(\lambda))$ as a function of $\log(\lambda)$ for this spectrum. The broken line is the linear regression through the points, yielding values of 1·67 for α and 0·625 for $\tau(500)$. The large values of $\tau(\lambda)$ at 730 and 770 nm are due to water vapour absorption bands centred at 730 and 760 nm. Because of these absorption bands and the weak oxygen absorption band at 690 nm, the wavebands 680–700 nm and 720–780 nm were omitted from the analysis of each spectrum. The coefficients α and $\tau(500)$ were found for each spectrum.

Values of α estimated by this method are influenced by the accuracy in measuring $I(\lambda)$, especially at small turbidities and large air-masses. An error in calibration could cause curvature of the graph of $\log(\tau(\lambda))$ against $\log(\lambda)$. Analysis of this effect (McCartney 1975) indicates that when $\tau(500)$ was greater than 0·2 and m was less than 3 ($Z < 70{\cdot}5°$) an uncertainty in spectroradiometer sensitivity of $\pm 5\%$ produced an uncertainty in α of less than $\pm 0{\cdot}2$. The maximum uncertainty in α was estimated to be about $\pm 0{\cdot}3$.

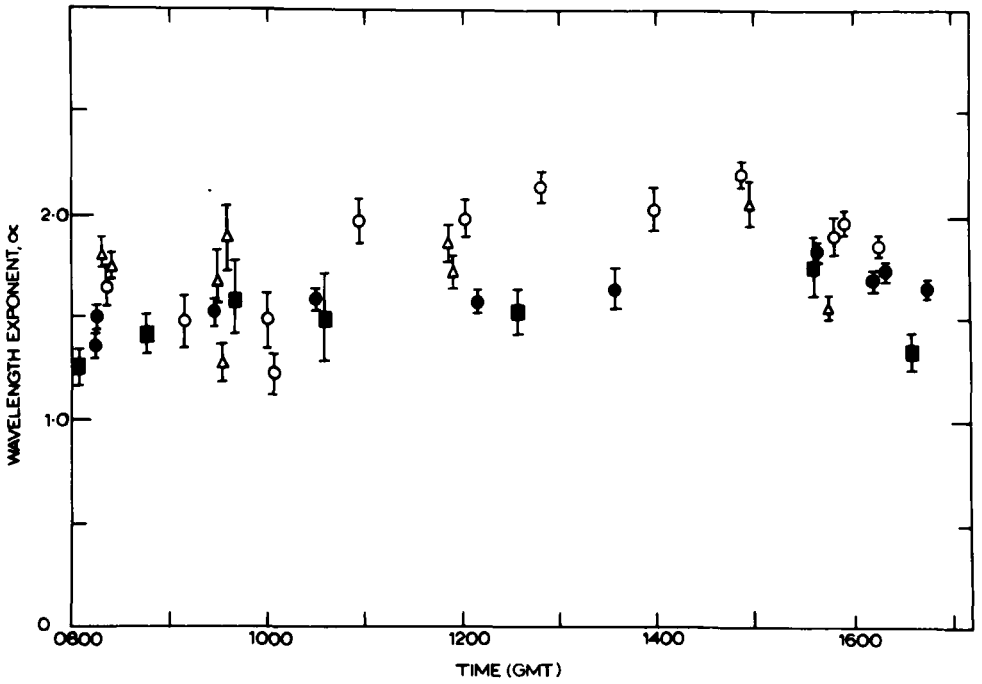

Figure 3. Diurnal variation in wavelength attenuation exponent, α, for 4 days, summer 1973. △ 5 June; ■ 15 June; ● 11 September; ○ 12 September.

Fig. 3 shows the diurnal variation of α for four individual days when the prevailing air mass was of continental origin. Scatter of the points is large in some cases, but the general trend is for a slight increase in α towards the afternoon.

Unsworth and Monteith (1972) showed that atmospheric turbidity (τ_t) at Sutton Bonington depended largely on the origin of the prevailing air mass. McWilliams (1973) showed that Ångstrom's turbidity coefficient was also dependent on wind direction and air mass origin at Valentia observatory in southwest Ireland. The measurements were therefore grouped into air masses of continental and maritime origin (77% and 17% respectively).

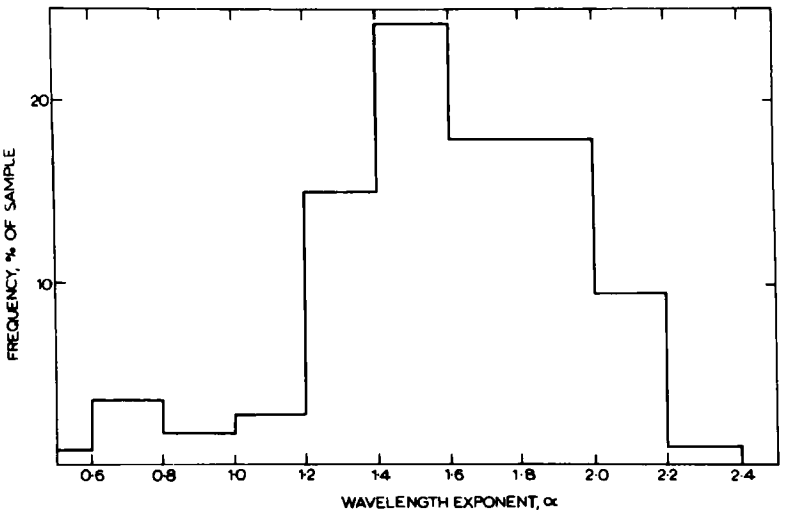

Figure 4. Frequency distribution of wavelength attenuation exponent, α: all measurements.

The frequency distributions of α for each type of air mass were not significantly different but this may be because of the relatively small number of measurements in maritime air. Figure 4 shows the distribution of α for all the spectral measurements. The mean value was 1·66 with a standard deviation of 0·35 the largest fraction lying in the range 1·4–1·6 (24%).

The frequency distributions of values of $\tau(500)$ in continental and maritime air masses are shown in Fig. 5. The samples were not large enough to detect significant differences in the distributions of $\tau(500)$ for different values of α. The mean value of $\tau(500)$ for maritime air was smaller than for continental air, 0·39 compared with 0·44. The small number of measurements in the maritime sample must be taken into account when comparing the distributions but the results appear to indicate that the value of $\tau(500)$ in maritime air tends to be smaller than in air of continental origin.

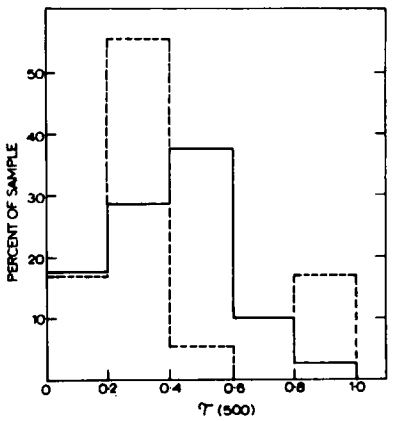

Figure 5. Frequency distribution of aerosol attenuation coefficient at 500 nm, $\tau(500)$. —— continental air; - - - - - maritime air.

(*b*) *Wideband results*

Integral turbidities in the wavebands 300–630 nm (τ_r), 300–710 nm (τ_v) and 300–3000 nm (τ_t) were calculated using Eq. (5) from measurements of direct solar irradiance in each waveband made using the pyrheliometer. The clear atmosphere irradiance, $I_*(\Delta\lambda)$, was calculated using the extraterrestrial solar spectrum of Thekaekara (1971) and the ozone and Rayleigh attenuation data of Elterman (1968). Water vapour and carbon dioxide absorption (applicable only in calculating τ_t) were calculated from knowledge of precipitable water in the atmosphere using the integral absorption coefficients of Yamamoto (1962). Precipitable water vapour was estimated from radiosonde data from an appropriate Meteorological Office station, Crawley, Aughton or Hemsby. Air-mass, m, and zenith angle, Z, were calculated using standard astronomical equations. The earth–sun distance correction was taken from McCulloch and Porter (1971).

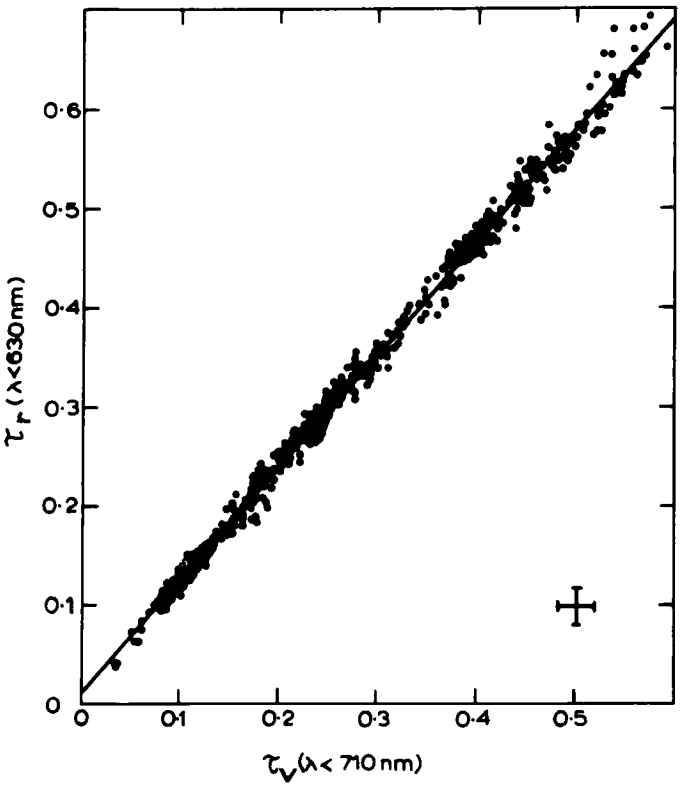

Figure 6. Measured relationship between τ_r and τ_v, Sutton Bonington, summer 1972 and 1973. The points are well fitted by the relationship $\tau_r = 1{\cdot}13\tau_v + 0{\cdot}012$.

Fig. 6 shows the measured relationship between τ_r and τ_v and represents over 500 individual measurements made on 54 days. The uncertainty in each measurement is indicated in the right hand corner of the figure. The relationship is well described by the linear equation $\tau_r = c\tau_v + d$, where $c = 1{\cdot}130$ and $d = 0{\cdot}012$ with standard errors of 0·005 and 0·002 respectively and regression coefficient of 0·997. Comparison of the measured slope c with the value of τ_r/τ_v in Fig. 1 indicates that the equivalent mean value of α is about 1·7. This is similar to the value of α found from spectral measurements ($\bar{\alpha} = 1{\cdot}66$).

Similar analyses were carried out for measurements made in air of continental and

maritime origin. As in the case of the spectral measurements, no significant difference was found between the relationships for each set of measurements. This may be due to the relative insensitivity of the method to small changes in α (e.g. $\pm 0{\cdot}5$).

The relationship between τ_t and τ_v shown in Fig. 7 is fitted by the line $\tau_t = e\tau_v + f$, with $e = 0{\cdot}64$ and $f = 0{\cdot}085$ with standard errors of 0·01 and 0·002 respectively and regression coefficient of 0·985.

The mean air-mass for all measurements was about 1·6 (zenith angle 45°) therefore Fig. 1 implies that the slope e corresponds to a mean α of about 1·3, apparently significantly smaller than indicated by measurements in the visible waveband.

The non-zero intercepts in both sets of experimental results are due to uncertainties in measuring I_v, I_r and I_t and in estimating I_{*v}, I_{*r} and I_{*t}. Detailed consideration shows that such errors should not influence the slope of the relationships at the air-masses and turbidities examined in this study.

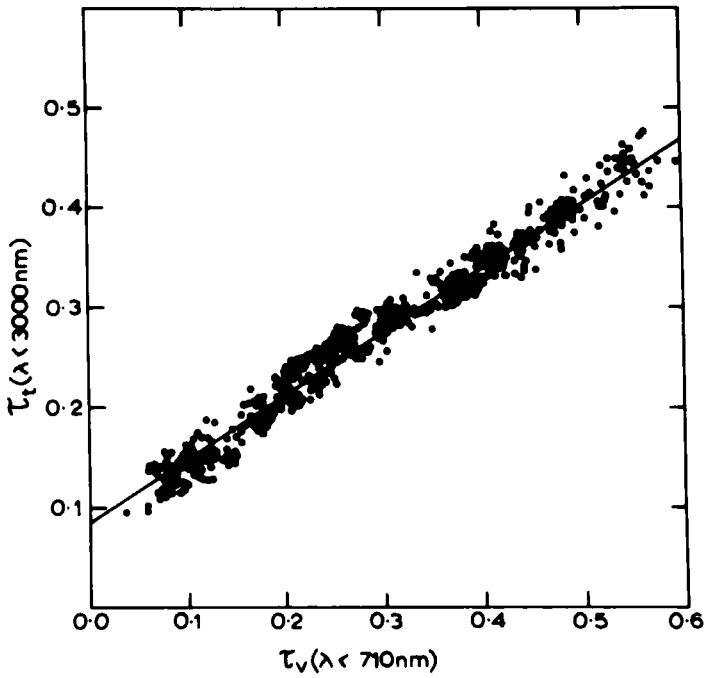

Figure 7. Measured relationship between τ_t and τ_v, Sutton Bonington, summer 1972 and 1973. The points are fitted by the relationship $\tau_t = 0{\cdot}64\tau_v + 0{\cdot}085$.

The difference in the values of α estimated from Figs. 6 and 7 can be explained in two ways. First, the slope e can be influenced by the scatter of circumsolar radiation into the aperture of the pyrheliometer resulting in an overestimation of I_v and I_t (i.e. an underestimation of τ_v and τ_t). As scattering is more predominant in the visible waveband, the error in τ_v will be greater than the error in τ_t making e too large (reducing α). Second, the value of α estimated from e assumes that $\tau(\lambda)$ follows a power law, with exponent α, throughout the waveband 300–3000 nm. There are indications that many aerosol constituents absorb significant amounts of radiation (Sheppard 1958; Robinson 1962) mainly in the infrared (Twitty and Weinman 1971; Volz 1972). If this is the case, then the absorption will have a greater effect in the total than in the visible waveband resulting in the measured values of τ_t being larger than those predicted by calculations which use the value of α estimated from measurements made in the visible waveband. Then, as τ_v remains almost

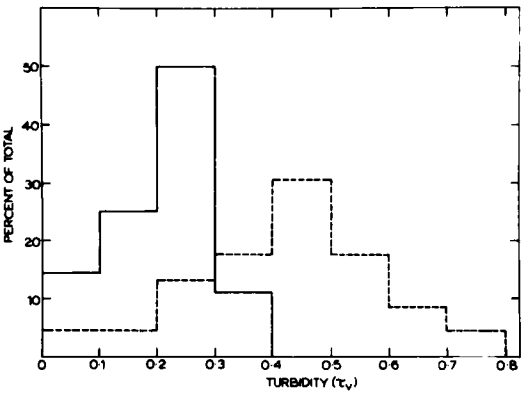

Figure 8. Frequency distribution of daily mean turbidity, $\bar{\tau}_v$, for 1972 and 1973. ----- continental air; —— maritime air.

unchanged, the measured slope e will be larger than calculations predict, resulting in a smaller estimation of α.

The results of Figs. 6 and 7 and the estimation of α from the spectral measurements are compatible if it is postulated that aerosol attenuation follows a power law in the visible waveband, with α about 1·7, but that attenuation is larger at infrared wavelengths than the power law predicts due to aerosol absorption.

To investigate the frequency distribution of occurrence of turbidity values, the mean visible turbidity, $\bar{\tau}_v$, was calculated for each day of measurements. The prevailing air mass was identified as being of maritime origin on 53% of the days and of continental origin on 43%. Figure 8 shows the relative frequency distribution of $\bar{\tau}_v$, in increments of 0·1, for both maritime and continental air. The distributions were significantly different, with mean values of 0·21 for maritime and 0·42 for continental. The continental values were approximately normally distributed with a standard deviation of 0·16. The maritime distribution was skewed towards larger values of $\bar{\tau}_v$, but the range of values covered was smaller than for the continental air. The mean value of $\bar{\tau}_v$ for all the days was 0·31.

Theoretical calculations using a simplified atmospheric model (McCartney 1975) indicated that $\tau(500)$ could be considered proportional to $\bar{\tau}_v$ for the range of turbidities studied, the constant of proportionality being approximately independent of α for $0 < \alpha < 2$, i.e.

$$\tau(500) = 1{\cdot}06\bar{\tau}_v \quad . \quad . \quad . \quad . \quad (6)$$

Substitution of the mean values of $\bar{\tau}_v$ into Eq. (6) yields $\tau(500) = 0{\cdot}445$ for continental air and $\tau(500) = 0{\cdot}223$ for maritime air. The mean value of $\tau(500)$ for continental air compares well with the value obtained from spectral measurements but the value for maritime air is lower, probably due to the small number of spectral measurements in maritime air.

Because of the difference in the turbidity distributions in continental and maritime air a more detailed analysis was carried out. Air masses over the United Kingdom can be classified into seven principal types. Figure 9 shows $\bar{\tau}_v$ as a function of air mass for 50 days during 1972 and 1973. Means and standard deviations are shown in Table 2. Polar maritime, Pm, and returning polar maritime, rPm, air tended to be less turbid than the others due probably to their long sea paths. The larger values of τ_v in arctic maritime, Am, air may be due to 'local' effects because the air mass trajectories passed over industrial areas of central Scotland and northern England before reaching the Midlands. Arctic continental and polar continental air were the most turbid having passed over large

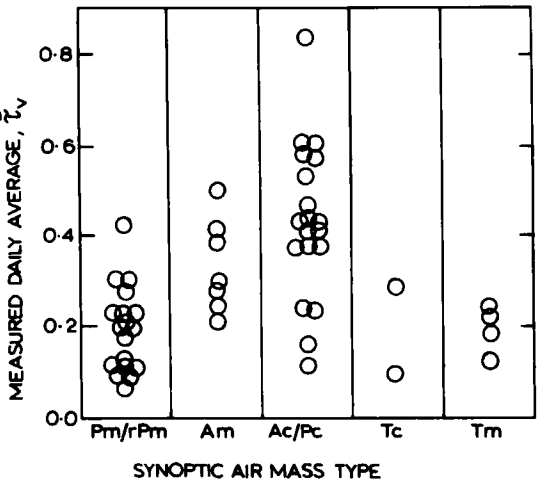

Figure 9. Measured daily mean τ_v classified by air mass.

industrial areas of northern Europe. Fig. 9 is in general agreement with the findings of Unsworth and Monteith (1972), Lovelock (1972) and McWilliams (1973) who all reported higher turbidities in air masses which had passed over continental Europe.

TABLE 2. AVERAGE DAILY MEAN VALUES OF τ_v FOR DIFFERENT AIR MASSES

Air mass	Mean $\bar{\tau}_v$	No. of days
Returning polar maritime (rPm)	0·26±0·04	6
Polar maritime (Pm)	0·13±0·05	11
Arctic maritime (Am)	0·31±0·06	6
Arctic/polar continental (Ac/Pc)	0·43±0·21	20
Tropical continental (Tc)	0·14±0·09	3
Tropical maritime (Tm)	0·20±0·06	5

(*c*) *Ratio of visible to total irradiance, ε_i*

For many biological and physical applications of radiation data it is useful to know the fraction, ε_i, of visible irradiance in the total solar waveband. Unsworth and Monteith (1972) examined the ratio of visible to total irradiance in the direct beam and found that it was linearly dependent on the integral turbidity coefficient, τ_i, for zenith angles less than 60°.

The value of ε_i depends on atmospheric aerosol content, atmospheric water vapour content and zenith angle. As the aerosol spectral attenuation was fairly constant for this set of observations a well-defined relationship between τ_v and ε_i can be expected. During the period of measurement the mean precipitable water vapour was 1·5 cm with a range from 0·8 to 2·5 cm. The energy absorbed by water vapour, CO_2 and oxygen, in the total waveband, is shown in Table 3 for precipitable water of 0·8, 1·5 and 2·5 cm and several atmospheric masses. The table shows that at a fixed air-mass the energy absorbed varies by only about $\pm 25 W m^{-2}$, which is equivalent to a change in ε_i of between 0·01 and 0·02 for moderate turbidities and air-masses. Thus the effect of the variation of water vapour on ε_i at fixed air-mass was small for average conditions during the period of study.

The ratio ε_i was calculated for all measurements and the results were analysed as

TABLE 3. WATER VAPOUR ABSORPTION ($W m^{-2}$)

Air-mass	Zenith angle (deg)	Precipitable water (cm) 0·8	1·5	2·5
1·0	0·0	139	166	188
2·0	60·0	168	198	219
3·0	70·5	188	221	243

Calculated from Yamamoto (1962).

functions of zenith angle and turbidity. Linear regressions were fitted to ε_i v. τ_v for four different zenith angle ranges: 30–40°, 40–50°, 50–60° and 60–70°. Table 4 lists the slopes, intercepts and regression coefficients for the four lines while the slopes and intercepts are shown as functions of zenith angle in Fig. 10. The results of a similar analysis of ε_i as a function of τ_i compare reasonably well with the findings of Unsworth and Monteith (1972). Fig. 10 can be used to estimate ε_i from arbitrary visible turbidity and zenith angle. The standard error of the estimate, defined as $\Delta\varepsilon_i = \pm(\tau_v \Delta k + \Delta l)$, where Δk and Δl are the standard errors in the slope and intercept (Table 4), is shown as a function of τ_v and zenith angle in Table 5.

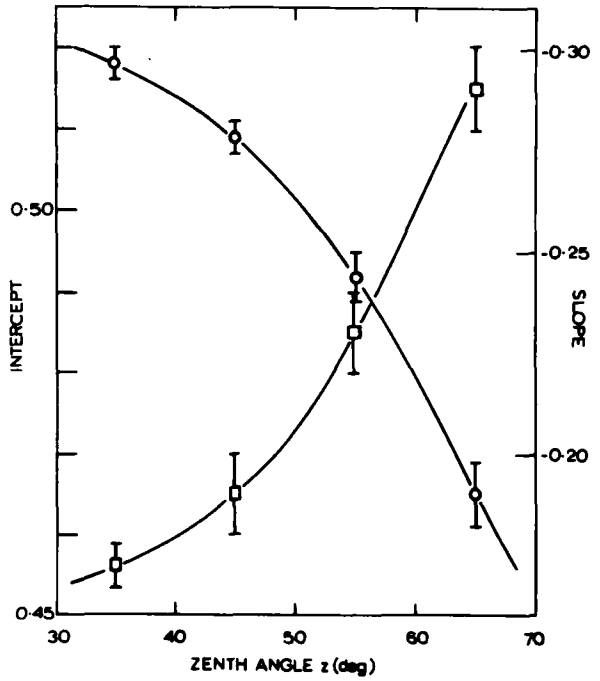

Figure 10. Relationship between slope and intercept of the linear regression between ε_i and τ_v and zenith angle. □ slope; ○ intercept.

TABLE 4. LINEAR REGRESSION FOR ε_i AS A FUNCTION OF τ_v

Zenith angle	Slope	Intercept	Regression coefficient	Number of points
30–40°	−0·172±0·005	0·518±0·002	0·96	135
40–50°	−0·19 ±0·01	0·509±0·003	0·92	131
50–60°	−0·23 ±0·01	0·492±0·003	0·90	136
60–70°	−0·29 ±0·01	0·465±0·004	0·93	91

TABLE 5. STANDARD ERROR IN ε_i AS A FUNCTION OF τ_v AND ZENITH ANGLE

Zenith angle (deg.)	τ_v 0·05	0·25	0·4
35	0·002	0·003	0·004
45	0·004	0·005	0·006
55	0·004	0·006	0·007
65	0·005	0·007	0·009

5. ESTIMATING DIRECT IRRADIANCE

(*a*) *Direct spectral irradiance*

Eq. (4) enables direct spectral irradiance to be calculated from turbidity and air-mass if the irradiance for a 'clean' atmosphere, $I_*(\lambda)$, is known (Table 1). The spectral turbidity coefficient, $\tau(\lambda)$, is generally adequately described by Eq. (2), α lying between 1·3 and 2·0 (section 4(*a*)). The constant γ is related to the aerosol attenuation coefficient at 500 nm by Eq. (3) and $\tau(500)$ generally lies between 0·1 and 0·8 in central England (sections 4(*a*) and 4(*b*)).

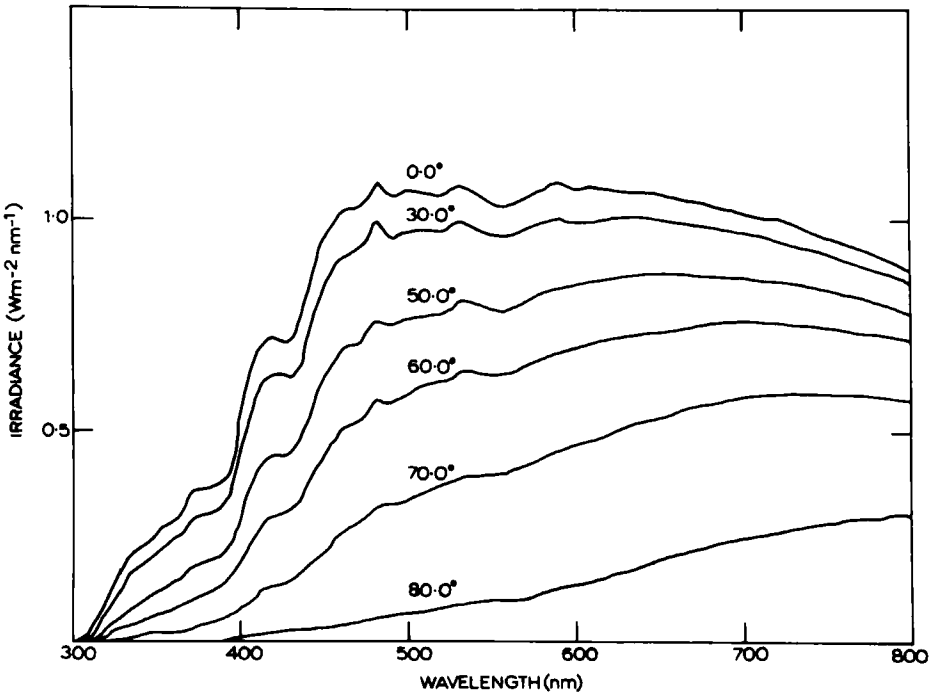

Figure 11. Spectral irradiance calculated for mean values of α and $\tau(500)$ (section 4(*a*)). Atmospheric ozone content = 0·35 cm. Zenith angle shown above each curve.

Use of Eq. (4) is illustrated in Fig. 11 which shows spectral irradiance calculated for the mean values of α and $\tau(500)$, reported in section 4(*a*), for several zenith angles. The weak oxygen and water vapour absorption bands at 690, 760 and 720 nm have not been allowed for in the calculations.

(*b*) *Direct irradiance in the visible and total wavebands*

Visible irradiance, I_v, can be similarly estimated from τ_v and zenith angle using Eq. (5)

if I_{*v} is known. For $m < 3$ ($Z < 70°$) clean atmosphere irradiance, ignoring ozone absorption, is well fitted by the polynomial

$$I_{*v} = 623{\cdot}9 - 118{\cdot}2m + 17{\cdot}7m^2 - 1{\cdot}88m^3 + 0{\cdot}12m^4 \,(\mathrm{W\,m^{-2}})$$

with an error of less than 2 $\mathrm{W\,m^{-2}}$.

From Table 4 or Fig. 10 the ratio of visible to total irradiance, ε_i, can be estimated for chosen values of τ_v and zenith angle, enabling I_t to be calculated from I_v.

6. Comparison with other measurements

There have been relatively few narrowband investigations of the attenuation of direct solar radiation by atmospheric aerosols (Curcio 1961; Ahlquist and Charlson 1969; Decker and Mahapatra 1975). Most investigations have been made using wideband measurements. The results are frequently reported in terms of Ångstrom's turbidity coefficient, β (Ångstrom 1964), or Schüeppe's coefficient, B (Valko 1961), but these may also be analysed to yield values of $\tau(500)$. If the wavelength dependence is assumed to follow a power law (Eq. (2)) the exponent α can be estimated from irradiance measurements made in two or more wavebands (Manes 1972; Hansen 1974). Many investigations using these techniques have been reported (Ångstrom 1964; Kuhn 1972; Rangarajan 1972; Manes 1972).

Table 6 shows mean values of α and $\tau(500)$ for several different locations. The mean value of α for Sutton Bonington falls within the range reported for Europe and North America, being slightly smaller than the values for remote or high altitude sites. Mean turbidity values are also within the range reported from European and American sites but

TABLE 6. Mean values of α and $\tau(500)$ for several sites

Site	α		$\tau(500)$		Source
	Mean	Range	Mean	Range	
Florida	1·3	0·65–1·9			Curcio and Durbin (1959)
Potsdam	2·0	1·2–2·6			Ångstrom (1964)
Davos	1·3	max 2·5			
Washington	1·8	1·2–2·5			Ahlquist and Charlson (1969)
U.S.A.					
Lat. 40–50°			0·18*		Volz (1969)
Lat. 30–40°			0·36*	0·06–1·8*	
Europe				0·2–0·5*	
France (Le Hougen)	1·3	0·1–2·4			Irvine and Peterson (1970)
South Africa (Boyden)	0·8	0·0–2·0			
Antarctica	1·8	0·8–3·2	0·042*	0·03–0·07*	Kuhn (1972)
India (Poona)	0·5	−0·5–1·4		0·14–0·46	Rangarajan (1972)
Jerusalem	1·3	0·2–3·6	0·14 (summer)* 0·07 (winter)*	0·05–0·41*	Manes (1972)
Ås (Norway)	2·13	0·9–3·3	0·11*	0·05–0·20*	Hansen (1973)
Potsdam	2·15		0·19*		
Davos	2·06		0·11*		
Stanleyville	1·65		0·41*		

* Estimated from Schüeppe's turbidity coefficient B.

TABLE 7. MEAN TURBIDITIES FROM SITES IN THE BRITISH ISLES

Site	τ_v Mean	τ_v Range	$\tau(500)$ Mean	$\tau(500)$ Range	Source
Strontian	0·11*				Unsworth and Monteith (1972)
Kew			0·3†	0·15–0·42	Stagg (1950)
Bowerchalk			0·41‡ (summer) 0·11‡ (winter)		Lovelock (1972)
Adrigole (Ireland)			0·18‡ (summer) 0·07‡ (winter)		
Valentia (Ireland)			0·12*	0·07–0·20	McWilliams (1973)
Sutton Bonington	0·31	0·1–0·7	0·44	0·20–1·00	This study

* Estimated from τ_t using relationship in section 4(*b*).
† Estimated from Ångstrom's turbidity coefficient (calculated assuming a value of $\alpha = 1{\cdot}3$).
‡ Estimated from Schüeppe's coefficient *B*.

are larger than at remote or high altitude sites where the air is expected to be cleaner.

There appears to have been no systematic investigation of spectral attenuation of solar radiation in the United Kingdom although several authors have reported sun and sky spectra, but usually in terms of colour temperature or in relative units (Henderson and Hodgkiss 1963). More attention has been paid to wideband irradiance, usually in the total waveband (Stagg 1950; Forbes and Hamilton 1971; Unsworth and Monteith 1972) but occasionally in narrower wavebands (Blackwell, Eldridge and Robinson 1954). Analysis of radiation data from Kew by Blackwell *et al.* showed that α lay in the range 0–1·5. Table 7 shows reported values of τ_v and $\tau(500)$ for several sites in the British Isles. For sites in central England turbidity values compare well with those reported here while remote or coastal sites have lower turbidities.

7. CONCLUSIONS

The measurements reported here suggest that in central England, in summer, spectral turbidity in the visible waveband can generally be described by a power law (Eq. (2)) with exponent about 1·7. This value is larger than that generally associated with natural aerosols, i.e. about 1·3 (Junge 1963). It has been shown that aerosol size distributions with relatively large fractions of particles less than 1000 nm produce attenuation spectra with large values of α (Valko 1961). There is evidence that particles (notably ammonium sulphate) produced by gas phase reactions of atmospheric pollutants are smaller than the majority of natural aerosol particles (Ludwig and Robinson 1968; Herd and Wiffin 1969). Large concentrations of ammonium sulphate particles have been reported in aerosols over the United Kingdom (Garland 1969; Eggleton 1969; Herd and Wiffin 1969) and Unsworth (1974) showed that daily mean turbidity at Sutton Bonington was correlated with sulphate ion concentration from a number of sites. It may therefore be postulated that the relatively large value of α reported here, is consistent with the existence of a natural aerosol modified by the addition of particulate pollution from man-made sources.

In section 4(*b*) it was suggested that the difference in the mean values of α estimated from visible (τ_v and τ_r) and total (τ_v and τ_t) waveband measurements could have been caused by aerosol absorption in the infrared. In the visible turbidity range, 0·2–0·6, the

required 'additional' absorption is estimated to be between 2% and 4% of I_{*t} at air-masses about 1·5 (i.e. 20–40W m^{-2}). Investigations of the wavelength dependence of absorption by aerosol particles indicate that generally 'natural' aerosol particles (mainly silicates) exhibit little absorption (Grams, Blifford, Gillette and Russel 1974) while many pollution particles show substantial absorption especially at infrared wavelengths, particularly carbonaceous particles (Twitty and Weinman 1971) and ammonium sulphate particles (Volz 1972). This is consistent with the above suggestion that the aerosol prevalent over the United Kingdom, in summer, contains a substantial fraction of 'man-made' particles.

The results also show that even under clear sky conditions there may be a considerable reduction in direct solar irradiance due to attenuation by atmospheric aerosol (e.g. a reduction from aerosol-free conditions of up to 55% in the visible and 40% in the total wavebands for the range of turbidities encountered in this study, Table 8). In addition the spectral distribution of direct irradiance in the visible may also be significantly altered, Fig. 11. This has additional implications for physical and biological systems which are spectrally sensitive. As an example, Table 8 shows the effect of increasing turbidity, at fixed air-mass (m = 1·305, Z = 40°), on the luminous efficiency of direct visible radiation (300–700 nm) defined as

$$K_v = \int_{300}^{700} 685 f(\lambda) I(\lambda)\, d\lambda \Big/ \int_{300}^{700} I(\lambda)\, d\lambda$$

where $f(\lambda)$ is the wavelength response of the standard human eye (Coulson 1975). For average continental air conditions (τ_v = 0·4, α = 1·7) luminous efficiency is about 14% greater than for aerosol-free conditions and about 12% greater for average maritime air conditions (τ_v = 0·2, α = 1·7). At large turbidities ($\tau_v \simeq 0{\cdot}4$) the luminous efficiency begins to decrease. This is because as turbidity increases, the wavelength of maximum spectral irradiance, λ_{max}, increases; at small turbidities λ_{max} is less than the wavelength of maximum response of the human eye (550 nm), at moderate turbidity and air-masses ($\tau_v m \simeq 0{\cdot}5$) λ_{max} is about 550 nm and at large turbidities it is greater than 550 nm.

As many biological responses to visible radiation are photochemical in nature, quantum flux is a more appropriate measure of radiation than energy flux. Quantum flux is dependent both on the quantity and the quality of radiation. For example, for the measured average

TABLE 8. EFFECT OF TURBIDITY ON VISIBLE LUMINOUS EFFICIENCY, K_v, AND QUANTUM FLUX, Q_v

τ_v	I_v (W m^{-2})	I_t (W m^{-2})	Q_v (10^{20}photon s^{-1}m^{-2})	Q_v/I_v (10^{18}photon s^{-1}W^{-1})	K_v (Lumen W^{-1})
0·0	466	906	12·5	2·69	230
0·2	359	750	9·75	2·73	235
0·4	276	629	7·40	2·76	262
0·6	213	535	6·08	2·81	245

value of α and at air-mass m = 1·3 the direct visible quantum flux, Q_v, below an aerosol-free atmosphere can be reduced by up to 51% for the range of turbidities found in this study (Table 8); this is slightly less than the reduction in visible irradiance. This result is a consequence of Eq. (2) as $Q(\lambda)$ is proportional to λ^{-1}. The ratio of quantum to energy flux is also of concern to biologists. The ratio in the direct beam increases slowly with increasing turbidity (5% increase from aerosol-free conditions to τ_v = 0·6 at m = 1·3, Table 8).

More than half the energy scattered from the direct beam by atmospheric particles, even under cloudless skies, may reach the earth as diffuse radiation. Scattered radiation

when added to the direct beam (global irradiance) generally reduces the effects of turbidity on the quantity and quality of solar radiation on a given surface. The relationship between turbidity and global and diffuse irradiance on a horizontal surface in central England will be treated in a subsequent paper.

ACKNOWLEDGMENTS

This work was supported by a grant from the Agricultural Research Council and a research studentship from the Natural Environmental Research Council (H. A. McCartney). The authors gratefully acknowledge the advice of Professor J. L. Monteith of the Department of Physiology and Environmental Studies, Nottingham University, School of Agriculture, Sutton Bonington, Leicestershire.

REFERENCES

Ahlquist, N. C. and Charlson, R. J. 1969 Measurement of the wavelength dependence of atmospheric extinction due to scatter, *Atmos. Environ.*, **3**, 551–564.

Ångstrom, A. 1929 On the atmospheric transmission of sun radiation and on dust in the air. I, *Geogr. Annlr.*, **2**, 156–166.

1930 On the atmospheric transmission of sun radiation. II, *Ibid.*, **3**, 130–159.

Ångstrom, A. K. 1964 The parameters of atmospheric turbidity, *Tellus*, **16**, 64–75.

Ångstrom, A. and Rodhe, B. 1966 Pyrheliometric measurements with special regard to circumsolar sky radiation, *Ibid.*, **18**, 25–33.

Annals of the International Geophysical Year 1958 Volume V, Part VI, *Radiation instruments and their measurement*, 365–464, Pergamon, London.

Avaste, O., Moldau, H. and Schifrin, K. S. 1962 Spectral distribution of direct solar and diffuse radiation, *Estonian Academy of Science Institute of Atmospheric Physics*, Vol. 3 (in Russian).

Barnhardt, E. A. and Streete, J. L. 1970 A method of predicting atmospheric aerosol scattering coefficients, *Appl. Opt.*, **9**, 1337–1344.

Bergstrom, R. W. 1972 Predictions of the spectral absorption and extinction coefficients of an urban air pollution aerosol model, *Atmos. Environ.*, **6**, 247–258.

Blackwell, M. J., Eldridge, R. H. and Robinson, G. D. 1954 Five years continuous recording of total and diffuse solar radiation at Kew Observatory, *Air Ministry Meteorological Research Committee*, London, MRP No. 895.

Coulson, K. L. 1975 *Solar and terrestrial radiation, methods and measurement*, Academic Press, New York.

Curcio, J. A. 1961 Evaluation of atmospheric aerosol particle size distribution from scattering measurements in the visible and infrared, *J. Opt. Soc. Am.*, **51**, 548–551.

Curcio, J. A. and Durbin, K. A. 1959 Atmospheric transmission in the visible region, *NRL Rept. 5368, U.S. Naval Research Laboratories*, Washington D.C.

Dave, J. V., Halpern, P. and Braslau, N. 1975 Spectral distribution of direct and diffuse solar energy received at sea-level of a model atmosphere, *I.B.M., Palo-Alto Scientific Center Data Processing Division, Rpt. No. G320–3332.*

Decker, W. L. and Mahapatra, A. K. 1975 Estimates of atmospheric attenuation of solar radiation at specific wavelengths, *Intern. J. of Biometeorology*, **19**, 14–20.

Diermendjian, D. 1963 Tables of Mie scattering cross-sections and amplitudes, *Rand Corporation Special Report* R–407–PR.

Diermendjian, D., Clasen, R. and Viezee, W. 1961 Mie scattering with complex index of refraction, *J. Opt. Soc. Am.*, **51**, 620–633.

Drummond, A. J. and Ångstrom, A. K. 1967 Solar radiation measurements on Mauna Loa (Hawaii) and their bearing on atmospheric transmission, *Sol. Energy*, **11**, 133–141.

Dunkelman, L. and Scolnik, R. 1959 Solar spectral irradiance and the vertical atmospheric attenuation in the visible and U.V., *J. Opt. Soc. Am.*, **49**, 356–367.

Eggleton, H.	1969	The chemical composition of atmospheric aerosols on Teeside and its relation to visibility, *Atmos. Environ.*, **3**, 355–372.
Elterman, L.	1968	U.V., visible and I.R. attenuation for altitudes to 50 km, *Environmental Research Paper 285, AFCRL–68–0158.*
Forbes, A. J. and Hamilton, R. A.	1971	Clear sky radiation measurements at Lerwick, *Quart. J. R. Met. Soc.*, **97**, 99–102.
Garland, J. A.	1969	Condensation on ammonium sulphate particles and its effect on visibility, *Atmos. Environ.*, **3**, 347–354.
Gates, D. M.	1966	Spectral distribution of solar radiation at the Earth's surface, *Science*, **151**, 523–529.
Grams, G. W., Blifford, I. H., Gillette, D. A., and Russel, P. B.	1974	Complex index of refraction of airborne soil particles, *J. Appl. Met.*, **13**, 469–471.
Hansen, V.	1973	Measurement of turbidity and precipitable water at Ås, *Meld. Norg. LandbrHøisk*, **52**, 1–12.
	1974	Determination of atmospheric turbidity parameters from spectral solar radiation measurements, *Arch. Met. Geophys. Bioklm.*, **22**, 301–308.
Henderson, S. F. and Hodgkiss, D.	1963	Spectral energy distribution of daylight, *Br. J. Appl. Phys.*, **14**, 125–131.
Herd, M. J. and Wiffin, R. D.	1969	Electron microscopy of natural aerosols and the identification of particulate ammonium sulphate, *Atmos. Environ.*, **3**, 337–340.
Hodge, P. W.	1971	Large decrease in clear air transmission of atmosphere 1·7 km above Los Angeles, *Nature*, **229**, 549.
Howard, J. N., Burch, D. E. and Williams, D.	1955	Near infrared transmission through synthetic atmospheres, *Geophys. Research Paper 46*, AFCRL–tr–55213, Bedford Mass.
Irvine, W. M. and Peterson, F. W.	1970	Observation of atmospheric extinction from 0·315–1·06 μm *J. Atmos. Sci.*, **27**, 62–69.
Junge, C. E.	1963	*Air chemistry and radioactivity*, Academic Press, New York.
Kattawar, G. W. and Plass, G. N.	1967	Electromagnetic scattering from absorbing spheres, *Appl. Opt.*, **6**, 1377–1382.
Knestrick, G. L., Cosden, T. H. and Curcio, J. A.	1962	Atmospheric scattering coefficients in the visible and infrared regions, *J. Opt. Soc. Am.*, **52**, 1010–1016.
Kondratyev, K. Ya.	1969	*Radiation in the atmosphere*, Academic Press, New York.
Kuhn, M.	1972	Die Spectrale Transparenz der Antarktischen Atmosphäre, Teil II, Messergebnisse und Analyse, *Arch. Met. Geophys. Bioklm.*, 20, 299–344.
Langley, S. P.	1881	The bolometer and radiant energy, *Proc. Am. Acad. Arts. Sci.*, **8**, 343–358.
Lovelock, J. E.	1972	Atmospheric turbidity and CCl_3F concentration in rural Southern England and Southern Ireland, *Atmos. Environ.*, **6**, 917–925.
Ludwig, F. L. and Robinson, E.	1968	Variation in the size distribution of sulphur containing compounds in urban aerosols, *Ibid.*, **2**, 13–23.
McCartney, H. A.	1975	Spectral distribution of solar radiation above and within crops, Ph.D. thesis, University of Nottingham, School of Agriculture.
McCormack, R. A. and Ludwig, F. L.	1967	Climatic modifications by atmospheric aerosols, *Science*, **156**, 1358–1359.
McCullough, E. C. and Porter, W. P.	1971	Computing clear day solar radiation spectra for the terrestrial ecological environment, *Ecology*, **52**, 1008–1015.
McDonald, J. E. M.	1960	Direct absorption of solar radiation by atmospheric water vapour, *J. Met.*, **17**, 319–328.
McWilliams, S.	1973	Atmospheric turbidity at Valentia Observatory, *Technical Note Number 36, Irish Meteorological Service*, Dublin.
Manes, A.	1972	Atmospheric turbidity over Jerusalem, *Series A Meteorological Notes Number 26, Israel Meteorological Research and Development Division*, Bet-Dagen.
Mie, G.	1908	Beiträge zur Optik trüber Medien, speziell kolloidaler Metallosungen, *Annln. Phys.*, **25**, 377–445.
Moon, P.	1940	Proposed standard solar radiation curves for engineering use, *J. Franklin Inst.*, **230**, 583–617.

Penndorf, R.	1956	New tables of Mie scattering functions for spherical particles, part 6, total Mie scattering coefficients for real refractive indices, *Geophysics Research Paper USAF Number 45*, AFCRL-TR-56-204(6).
Penndorf, R. B.	1957	Refractive index for standard air and Rayleigh scattering coefficients for the spectral region between 0·2 and 20μm and their application to atmospheric optics, *J. Opt. Soc. Am.*, *47*, 176–182.
Quenzel, H.	1970	Determination of size distribution of atmospheric aerosol particles from spectral solar radiation measurements, *J. Geophys. Res.*, **75**, 2915–2921.
Randerson, D.	1970	A comparison of the spectral distribution of solar radiation in a polluted and a clear air mass, *J. Air Pollut. Control Ass.*, **20**, 546–548.
Rangarajan, S.	1972	Wavelength exponent of haze scattering in the tropics as determined by photoelectric photometers, *Tellus*, **24**, 56–64.
Rensch, D. B. and Long, R. K.	1970	Comparative studies of extinction and scattering by aerosols, fogs and rain at 10·6 and 0·63μm, *Appl. Opt.*, **9**, 1563–1573.
Roach, W. T.	1961	The absorption of solar radiation by water vapour and carbon dioxide in a cloudless atmosphere, *Quart. J. R. Met. Soc.*, **87**, 364–373.
Robinson, G. D.	1962	Absorption of solar radiation by atmospheric aerosol as revealed by measurements at the ground, *Arch. Met. Geophys. Bioklm.*, **12**, 19–40.
Robinson, N.	1966	*Solar radiation*, Elsevier, Amsterdam.
Schüeppe, W.	1949	Die Bestimmung der Komponenten Atmospharischen Trübung aus Aktometer-messangen, *Arch. Met. Geophys. Bioklm.*, **1**, 257–346.
Sheppard, P. A.	1958	The effect of pollution on radiation in the atmosphere, *Int. J. Air Pollut.*, **1**, 31–43.
Stagg, J. M.	1950	Solar radiation at Kew Observatory, *Meteorological Office Geophysics Memoirs No. 86*, MO 530a, 3–37.
Taylor, A. H. and Kerr, G. P.	1941	The distribution of energy in the visible spectrum of daylight, *J. Opt. Soc. Am.*, **31**, 3–8.
Thekaekara, M. P.	1971	Solar electromagnetic radiation, *NASA Space Vehicle Design Criteria (environment)*, NASA SP-8005.
Twitty, J. T. and Weinman, J. A.	1971	Radiative properties of carbon aerosols, *J. Appl. Met.*, **10**, 725–731.
Unsworth, M. H.	1974	Radiation measurements as indicators of natural and man-made aerosols, *W.M.O. Special Report* 3, *Observation and Measurement of Atmospheric Pollution*, 423–433.
Unsworth, M. H. and Monteith, J. L.	1972	Aerosol and solar radiation in Britain, *Quart. J. R. Met. Soc.*, **98**, 778–797
Unsworth, M. H. and McCartney, H. A.	1973	Effects of atmospheric aerosols on solar radiation, *Atmos. Environ.*, **7**, 1173–1185.
Valko, P.	1961	Untersuchung über die vertikale Trubungsschichtung der Atmosphäre, Ph.D. thesis, University of Budapest.
Van de Hulst, H. C.	1959	*Light scattering by small particles*, Wiley, New York.
Vittori, O., Tomasi, C. and Guzzi, R.	1974	Dessen's droplets in the near and middle infrared spectrum of the sun, *J. Atmos. Sci.*, **31**, 261–270.
Volz, F. E.	1969	Some results of turbidity networks, *Tellus*, **21**, 625–630.
	1972	Infrared absorption by atmospheric aerosol substances, *J. Geophys. Res.*, **77**, 1017–1031.
Yamamoto, G.	1962	Direct absorption of solar radiation by atmospheric water vapour, carbon dioxide and molecular oxygen, *J. Atmos. Sci.*, **19**, 182–188.
Yamamoto, G. and Tanaka, M.	1969	Determination of aerosol size distribution from spectral attenuation measurements, *Appl. Opt.*, **8**, 447–453.